

## Spin relaxation in InAs nanowires studied by tunable weak antilocalization

A. E. Hansen, M. T. Björk,\* C. Fath, C. Thelander, and L. Samuelson

*Solid State Physics/Nanometer Consortium, Lund University, P.O. Box 118 Lund, Sweden*

(Received 29 June 2004; revised manuscript received 11 February 2005; published 31 May 2005)

We report on a low-temperature magnetoconductance study to characterize the electrical and spin transport properties of *n*-type InAs nanowires grown by chemical beam epitaxy. A gate-controlled crossover from weak localization to weak antilocalization is observed. The measured magnetoconductance data agrees well with theory for one-dimensional quasi-ballistic systems and yields a spin relaxation length which decreases with increasing gate voltage.

DOI: 10.1103/PhysRevB.71.205328

PACS number(s): 73.63.-b, 72.25.Rb, 72.20.-i

### I. INTRODUCTION

In the field of spintronics,<sup>1,2</sup> spin physics is studied in electrical transport and optics experiments, and novel spin-based electronic devices are explored. Semiconductors play an important role in this field, e.g., due to the possibility of gate voltage manipulation of electron spins. For instance, electric field control of spin-orbit effects and spin precession have been demonstrated in two-dimensional semiconductor systems.<sup>3,4</sup> In one dimension, spin-orbit effects are predicted to be enhanced as a result of electron-electron interactions.<sup>5</sup>

Semiconductor nanowires belong to a new class of bottom-up fabricated nanoscale systems. Recent results have shown that nanowires can be of high crystalline quality, can have predefined lateral sizes down to 2 nm, and allow for heterostructure material combinations that are not possible in bulk semiconductors.<sup>6</sup> These remarkable characteristics make semiconductor nanowires promising for electronic and optical device applications,<sup>7-9</sup> however, spin effects in nanowire transport have not been explored. Determination of spin lifetimes is essential for the design of spin-based devices, and gives information on the fundamental spin transport mechanisms. Here, we report on a low-temperature magnetoconductance study to characterize the electrical and spin transport properties of InAs semiconductor nanowires.

Spin relaxation can be probed via magnetoconductance measurements. In disordered conductors at low temperatures, constructive interference of pairs of backscattered, time-reversed paths results in a negative weak localization (WL) correction to the conductivity.<sup>10</sup> In the presence of spin relaxation, the interference can be destructive,<sup>11</sup> yielding a positive conductivity correction known as weak antilocalization (WAL).<sup>12,13</sup> The conductivity correction disappears when a magnetic field sufficient to dephase time-reversed paths is applied. The magnetoconductivity correction depends on the length scales over which phase- and spin-information is preserved. In the InAs nanowires, we find a gate-voltage controlled WAL-WL crossover. Comparisons with diffusive<sup>10</sup> and quasi-ballistic<sup>14</sup> theories for the magnetoconductance of one-dimensional (1D) systems show that the crossover is due to a change in the relative sizes of the phase and spin coherence lengths; for shorter phase (spin) coherence length, weak localization (weak antilocalization) is observed. The extracted spin relaxation length in the 1D nanowires is  $\sim 200$  nm and tends to decrease with increasing

gate voltage. We discuss various mechanisms, including spin-orbit coupling, which can lead to spin relaxation. A gate-controlled crossover from WAL to WL has earlier been reported for 2D systems<sup>15-17</sup> and open quantum dots,<sup>18</sup> but to our knowledge not for quantum wires.

### II. EXPERIMENT

The InAs nanowires studied here were catalytically grown in the  $\langle 111 \rangle$  direction from 55 nm Au nanoparticles by chemical beam epitaxy. Details of the fabrication procedure can be found elsewhere.<sup>19</sup> The wires are  $\sim 2 \mu\text{m}$  long and  $60 \pm 4$  nm in diameter with virtually no tapering. Transmission electron microscopy investigations show that the wires are single crystalline although with a varying number of twin planes, which might affect the electron mean free path at low temperatures. Subsequent to growth, wires are transferred to a degenerately doped Si substrate with a 1000 Å SiO<sub>2</sub> layer. After locating individual wires, electrical contacts with an electrode spacing of 1.2  $\mu\text{m}$  were defined using electron beam lithography and metal evaporation (see inset of Fig. 1). The contacts were not annealed.

Electrical measurements were performed in a He-3 system in a perpendicular magnetic field. The conductance of

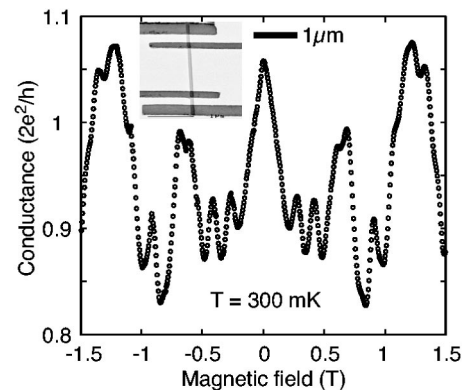


FIG. 1. The magnetoconductance trace at 300 mK and zero gate voltage for a single nanowire measured in a four-point configuration (inset shows a scanning electron image of the device). The presence of conductance fluctuations indicates a short elastic scattering length and the symmetry in magnetic field reflects a high transparency of the metal contacts to the wire.

individual wires is a few  $e^2/h$  at temperatures from 300 mK to  $\sim 100$  K. Above 100 K the resistance increases linearly with increasing temperature due to electron-phonon scattering. All measurements reported here were done below 100 K.

By applying a voltage to the Si substrate it is possible to gate the wires and previous measurements have demonstrated an  $n$ -type behavior.<sup>19</sup> One likely origin of the donors is carbon, incorporated from the metal-organic sources during growth. We note that those donors are not spatially separated from the conducting channel and could reduce the elastic scattering length. Another possible source of carriers is surface accumulation of electrons, known to appear for bulk InAs. Typically, the wires will be pinched off at a gate voltage of  $-3$  to  $-4$  V at low temperatures.

We first discuss four-point measurements on a single InAs nanowire. The conductance as a function of perpendicular magnetic field is displayed in Fig. 1, with the wire and metallic contacts shown in the inset. For temperatures lower than 20 K, universal conductance fluctuations (UCFs) are observed as a function of magnetic field, suggesting that the elastic scattering length is shorter than the wire length. UCFs are also observed in zero magnetic field when the gate voltage is changed. Below  $T \sim 1$  K the UCF amplitude saturates, which we interpret as a result of the phase coherence length reaching the size of the sample. The UCF signal in Fig. 1 is symmetric in magnetic field, which implies a high contact transparency. Consistently, the difference in resistance between a two- and a four-point measurement configuration is less than 2%. This is always observed for our InAs wire devices,<sup>20</sup> and in the following we use the two-point configuration.

The peak in the conductance at zero magnetic field suggests weak antilocalization due to the strong spin-orbit interaction in InAs. The presence of the UCF makes it difficult to determine the correction to the conductivity due to WAL or WL. To average out the UCF and determine the localization effects at small magnetic fields, we used a configuration consisting of nanowires connected in parallel.

The conductance as a function of gate voltage for 45 parallel wires is displayed in Fig. 2(a). Below  $-3$  V, the wires start to become pinched off and the exact number of wires contributing to transport is not known anymore. In Fig. 2(b) the magnetoconductance of the 45 parallel wires is shown for different voltages applied to the back gate. Measurements were performed at a temperature of 8 K in order to stay in the regime where the phase coherence length is shorter than the wire length. This has the additional advantage of reducing the UCF even further.

The crossover from WAL to WL as the carrier concentration is decreased by the back gate, shown in Fig. 2(b), is the main feature of the present work. Known theoretical expressions for the WL and WAL conductivity corrections are used to fit the data, as will be explained below.

Finally, the temperature dependence of the magnetoconductance for zero applied gate voltage is shown in Fig. 3. Again a crossover from WAL to WL is observed as the temperature is raised, as will be discussed later.

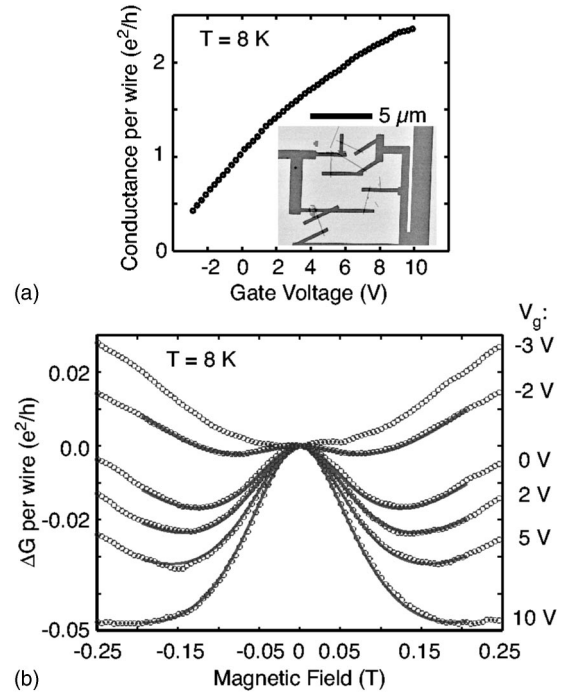


FIG. 2. (a) The average conductance per wire, measured on an array of 45 InAs nanowires connected in parallel, at a temperature of 8 K. Below  $-3$  V, the wires start to pinch off and consequently measurements were only done for larger gate voltages. The inset shows a scanning electron microscopy image of several wires with electrical contacts. In (b) the magnetoconductance, offset to zero at zero magnetic field, is plotted for six different gate voltages at a temperature of 8 K (open circles). A crossover from WAL to WL takes place as the gate voltage is decreased. Lines are fits to Eq. (3), explained in Sec. III.

### III. MODELING

We now compare the measured magnetoconductance data of the 45 parallel wires to two theoretical expressions for the conductivity correction due to WL/WAL in order to extract transport parameters. We consider only one-dimensional theory, meaning that the phase coherence length  $l_\phi \gg W$ , where  $W$  is the wire width.

One-dimensional theory assumes the phase coherence length to be much smaller than the wire length ( $l_\phi \ll L$ ) and

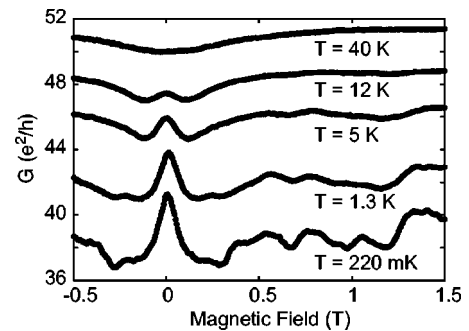


FIG. 3. The temperature dependence of the magnetoconductance at zero gate voltage for 45 wires connected in parallel. A crossover from WAL to WL occurs as the temperature is increased beyond 20 K. At low temperatures conductance fluctuations appear.

the Fermi wavelength to be much smaller than the wire width ( $\lambda_F \ll W$ ). From previous measurements<sup>21,22</sup> we have inferred values of the carrier concentration from  $10^{17}$  to  $10^{18}$  cm<sup>-3</sup> at zero gate voltage, resulting in a  $\lambda_F$  from 30 to 15 nm.<sup>23</sup> Also, the theory is valid only for small magnetic fields such that the magnetic length  $l_m = \sqrt{\hbar/eB}$  exceeds the wire diameter ( $l_m \gg W$ ). We therefore restrict the fitting to magnetic fields  $|B| < 0.2$  T, where  $l_m \gg W$ .

In the case of very small elastic scattering lengths ( $l_e \ll W$ , “dirty” limit) the following expression for the conductance correction  $\Delta G(B)$  is applicable:<sup>10,24</sup>

$$\Delta G(B) = -\frac{2e^2}{hL} \left[ \frac{3}{2} \left( \frac{1}{l_\phi^2} + \frac{4}{3l_{so}^2} + \frac{1}{D\tau_B} \right)^{-1/2} - \frac{1}{2} \left( \frac{1}{l_\phi^2} + \frac{1}{D\tau_B} \right)^{-1/2} \right]. \quad (1)$$

Here, we have assumed that the spin relaxation is due to spin-orbit effects, with a relaxation length  $l_{so}$ .<sup>25</sup>  $\tau_B$  is given by

$$\tau_B = \frac{3l_m^4}{W^2 D}, \quad (2)$$

where  $D$  is the diffusion constant.

On the other hand, if  $l_e \gg W$  (“pure” limit) flux cancellation has to be taken into account, and Eq. (1) is modified to<sup>14,24</sup>

$$\Delta G(B) = -\frac{2e^2}{hL} \left[ \frac{3}{2} \left( \frac{1}{l_\phi^2} + \frac{4}{3l_{so}^2} + \frac{1}{D\tau_B} \right)^{-1/2} - \frac{1}{2} \left( \frac{1}{l_\phi^2} + \frac{1}{D\tau_B} \right)^{-1/2} - \frac{3}{2} \left( \frac{1}{l_\phi^2} + \frac{1}{l_e^2} + \frac{4}{3l_{so}^2} + \frac{1}{D\tau_B} \right)^{-1/2} + \frac{1}{2} \left( \frac{1}{l_\phi^2} + \frac{1}{l_e^2} + \frac{1}{D\tau_B} \right)^{-1/2} \right], \quad (3)$$

where  $\tau_B$  is now

$$\tau_B = \frac{C_1 l_m^4 l_e}{W^3 D} + \frac{C_2 l_m^2 l_e^2}{W^2 D}. \quad (4)$$

The constants  $C_1$  and  $C_2$  depend on whether the boundary scattering in the nanowires is diffusive or specular. None of our experimental data suggest diffusive boundary scattering as observed for instance in wires defined by gating a two-dimensional electron gas.<sup>26</sup> Therefore we take  $C_1 = 19/2$  and  $C_2 = 24/5$ , appropriate for specular scattering.<sup>14</sup> No surface depletion is expected for InAs, and consequently we fix  $W$  to the measured wire diameter. Fitting parameters are thus  $l_\phi$  and  $l_{so}$  for the “dirty” limit expression Eq. (1) and  $l_\phi$ ,  $l_e$ , and  $l_{so}$  for the “pure” limit, Eq. (3). In Fig. 2(b) the model of Eq. (3) is fitted to data for five different gate voltages. A comparison between the models of Eq. (1) and Eq. (3) is made in Fig. 4. Both models describe the measured data reasonably well, however, the “pure” limit gives a better fit for all gate voltages, and a much better fit for  $V_g > 5$  V. We will therefore mostly refer to the results obtained from fits to the “pure” model in the following discussion. The fitting parameters obtained for both models at several gate voltages are

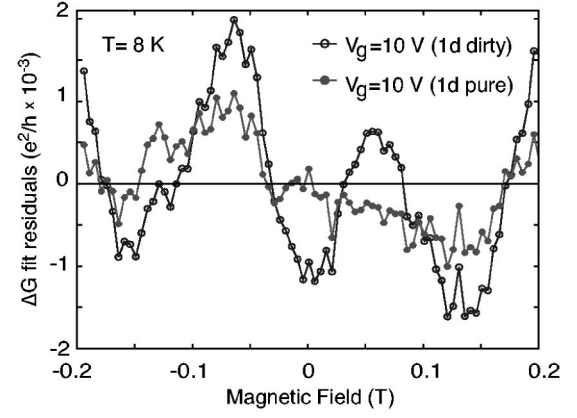


FIG. 4. We compare the two models used, Eq. (1) (dirty limit) and Eq. (3) (pure limit), by showing the difference between the fitted curves and measured conductance as function of magnetic field for 45 parallel wires. As an example the data measured at a gate voltage of 10 V is shown. At this gate voltage, we observe the largest differences between fits and data.

shown in Fig. 5. We observe that the basic requirements  $W < l_\phi < L$  and  $l_e < L$  of 1D theory are fulfilled.

#### IV. DISCUSSION

The transport parameters extracted from the measurements using the two theoretical expressions Eq. (1) and Eq. (3) for the conductance correction are shown in Fig. 5. Generally we note that the elastic scattering length  $l_e$  is larger than, but comparable to, the wire diameter  $W = 60$  nm, which is inconsistent with the assumption of either model ( $l_e \ll W$  or  $l_e \gg W$ ). Further, for a 2D system,<sup>27</sup> it was found that in the presence of spin-orbit interaction, an accurate determination of transport parameters requires a model that takes into account that different effects leading to conduction band spin splitting will not give additive spin relaxation rates. The models for the WL/WAL corrections used here only take

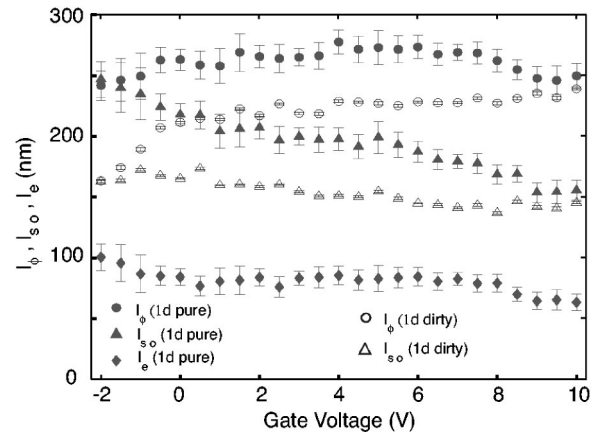


FIG. 5. The parameters extracted from the fits to the measured magnetoconductance obtained at 8 K, as a function of voltage applied to the back gate. The filled symbols are obtained using Eq. (3) (pure limit) and the open symbols using Eq. (1) (dirty limit). The error bars display the standard deviations of the fits.



spin-orbit coupling into account via a single spin relaxation length. Therefore, even if the models can describe the data reasonably well and give comparable parameter values, the precision of the values might be limited. We proceed to discuss the parameters shown in Fig. 5.

(a) *Elastic scattering length* An independent assessment of  $l_e$  is difficult since conventional four-point measurements to determine longitudinal and transverse resistivities cannot presently be carried out on our system. The extracted value of  $l_e$  and the above-mentioned values for the carrier concentration yield a resistance of 5–25 k $\Omega$ , consistent with the measurements [Fig. 2(a)]. Local gating of InAs nanowires with a gate width of 100 nm can result in signatures of conductance quantization,<sup>20</sup> giving an approximate lower bound for the elastic scattering length, also consistent with the value obtained here. We remark that optimization of growth conditions might enhance the purity of the nanowires.

(b) *Phase coherence length* The obtained value of the phase coherence length is  $\sim 260$  nm at a temperature of 8 K, corresponding to a phase coherence time  $\tau_\phi$  of 0.5–1 ps. This value can be compared with, e.g., the 100 ps observed in chaotic quantum dots in GaAs/GaAlAs heterostructures at  $T=1$  K,<sup>18</sup> and the  $\sim 50$  ps at  $T=0.4$  K in wires fabricated on GaAs/GaAlAs and GaInAs/AlInAs heterostructures.<sup>24</sup>

(c) *Spin relaxation length* The crossover from WAL to WL as shown in Fig. 2(b) occurs as  $l_{so}$  becomes equal in magnitude to  $l_\phi$  at low gate voltages. We proceed to estimate the importance of two well-known mechanisms that can lead to spin relaxation.<sup>2</sup>

In systems without inversion symmetry, spin splitting of the conduction band occurs due to spin-orbit coupling, which in combination with momentum scattering gives rise to spin relaxation. The *Dresselhaus effect*<sup>28</sup> due to bulk inversion asymmetry leads to splitting terms in the Hamiltonian of zinc-blende crystals which are cubic in wave vector  $k$ . In 2D, linear terms appear due to the confinement.<sup>2</sup> We are not aware of explicit calculations for the 1D case, but note that the spin splitting is absent in the  $\langle 111 \rangle$  direction of the present nanowires,<sup>28</sup> which should lead to a suppression of this scattering mechanism. For an approximate lower bound of the spin relaxation length, we can take the bulk value which is  $l_{so,D} = \hbar^2 [m^* k_F \gamma]^{-1} \sim 1-6 \mu\text{m}$ , which is longer than the measured spin relaxation length. We have used the effective mass  $m^* = 0.023m_e$  and  $\gamma = 27 \text{ eV \AA}^3$ , which are the values for bulk InAs.<sup>27</sup> The wave vector  $k_F$  is estimated from the above quoted electron density at zero gate voltage. As this lower bound for  $l_{so}$  is much larger than the deduced values shown in Fig. 5, we conclude that the Dresselhaus effect does not play a role in our experiment. The *Rashba effect*<sup>29</sup> due to structural inversion asymmetry also leads to a  $k$ -linear spin splitting term giving an approximate relaxation length  $l_{so,R} = \hbar^2 (m^* e E \alpha_o)^{-1}$ . Here  $E$  is an electric field across the wire, which could arise from the asymmetric gate coupling. The value for  $\alpha_o$  for bulk InAs is<sup>27</sup>  $117 \text{ \AA}^2$ . The measured spin-orbit length of  $\sim 200$  nm corresponds to  $\alpha = e E \alpha_o \sim 1.6 \times 10^{-11} \text{ eV m}$ , which implies a voltage drop  $EW$  across the wire of 0.8 V, or twice the energy gap of InAs. We find this value surprisingly large, and note that, theoretically, the determination of  $\alpha$  can be nontrivial.<sup>2</sup> However, we also note that electron-electron

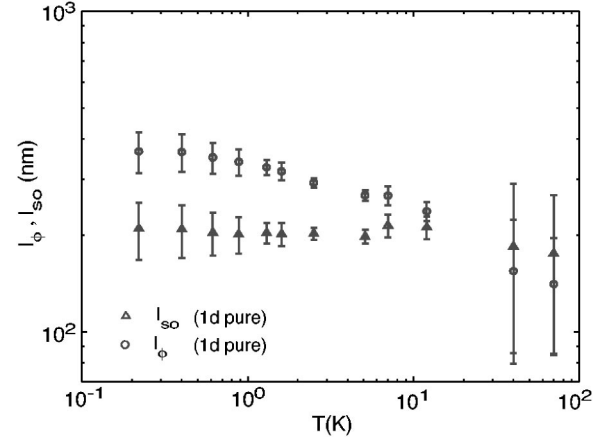


FIG. 6. The parameters extracted from the fits to the measured data at zero gate voltage, as a function of temperature. Fits to the data were done according to Eq. (3) (pure limit). The crossover from WAL to WL, seen at high temperature in Fig. 3, occurs when the phase coherence becomes smaller than the spin relaxation length. The error bars display the standard deviations of the fits.

interaction can enhance spin-orbit effects.<sup>5</sup> Experimentally, a value  $\alpha \sim 10^{-11} \text{ eV m}$  was found in InGaAs/InAlAs heterostructures.<sup>3</sup>

Spin relaxation can also occur via the *Elliott-Yafet mechanism*.<sup>30</sup> Here momentum scattering gives rise to spin relaxation due to spin-splitting of the valence band. The resulting bulk spin relaxation length, computed in a three-band  $k \cdot p$ -approximation,<sup>31</sup> is  $l_{EY} = \sqrt{3/8} (E_g/E_F) l_e (E_g + \Delta_{so}) (3E_g + 2\Delta_{so}) [\Delta_{so} (2E_g + \Delta_{so})]^{-1} = 0.5-2 \mu\text{m}$ . Here  $E_g = 0.42 \text{ eV}$  is the band gap, and  $\Delta_{so} = 0.38 \text{ eV}$  is the valence band splitting of InAs. Hence this mechanism could be of importance in our system.

Other mechanisms of spin relaxation exist, such as scattering on paramagnetic impurities. However, the possible source of those impurities is unclear; the metal contacts to the wires do contain Ni but are not annealed, so Ni should not diffuse into the wires.

To summarize, from our simple numerical estimates, we have found that the Elliott-Yafet mechanism may account for the magnitude of the experimentally observed spin relaxation length. For the Rashba spin-orbit splitting, large electric fields across the wire are needed to explain the observed spin relaxation length. We note that both the Elliott-Yafet mechanism and the Rashba and Dresselhaus effects predict a spin-orbit relaxation length that is decreasing with increasing gate voltage, as is observed in Fig. 5.

Finally, the data taken at temperatures from 0.2 to 70 K were also fitted using Eq. (3). The results are shown in Fig. 6 and demonstrate how the phase coherence length increases with decreasing temperature until it saturates at  $\sim 1$  K. The spin relaxation length remains constant in the entire temperature interval. Around 20 K  $l_\phi$  becomes equal to the spin relaxation length resulting in the crossover from WL to WAL.

## V. CONCLUSIONS

We have reported the observation of a gate-voltage-controlled crossover from WL to WAL in InAs semiconduc-

tor nanowires, demonstrating the influence of spin relaxation on transport. We have compared the measured magnetoconductance with theory for 1D diffusive and quasi-ballistic systems. Quasi-ballistic theory gives the better fit to our data and yields an elastic scattering length of 60–100 nm, slightly larger than the wire diameter. From the fits, the spin relaxation length is found to be of the order of 200 nm and tends to decrease with increasing back gate voltage.

Rashba spin-orbit effect could be responsible for the observed spin relaxation, if the asymmetric gate coupling gives rise to a large electric field across the wire. A detailed investigation of our particular geometry, a semiconductor wire on a SiO<sub>2</sub>/Si substrate, is needed to address this issue. Also, the Elliott-Yafet spin relaxation mechanism could probably be relevant in our system due to the small bandgap and large

valence band spin-orbit splitting of InAs. Finally, we emphasize that the models for the WL/WAL corrections used here only take spin-orbit coupling into account via a single spin relaxation length, which is not adequate if more than one spin-orbit effect contributes to the conduction band spin splitting.<sup>27</sup> Theoretical work addressed at band structure spin splitting and WL/WAL correction in 1D semiconductor systems is needed for further investigations of spin transport in nanowires.

#### ACKNOWLEDGMENTS

This work was supported by the Swedish Foundation for Strategic Research (SSF), the Swedish Research Council (VR), and Office of Naval Research (ONR).

---

\*Corresponding author. Electronic address: mikael.bjork@ftf.lth.se

<sup>1</sup>S. A. Wolf, D. D. Awschalom, R. A. Buhrman, J. M. Daughton, S. von Molnár, M. L. Roukes, A. Y. Chtchelkanova, and D. M. Treger, *Science* **294**, 1488 (2001).

<sup>2</sup>I. Zutic, J. Fabian, and S. Das Sarma, *Rev. Mod. Phys.* **76**, 323 (2004).

<sup>3</sup>J. Nitta, T. Akazaki, H. Takayanagi, and T. Enoki, *Phys. Rev. Lett.* **78**, 1335 (1997).

<sup>4</sup>Y. Kato, R. C. Myers, A. C. Gossard, and D. D. Awschalom, *Nature (London)* **427**, 50 (2004).

<sup>5</sup>W. Häusler, *Phys. Rev. B* **63**, 121310(R) (2001).

<sup>6</sup>M. T. Björk, B. J. Ohlsson, T. Sass, A. I. Persson, C. Thelander, M. H. Magnusson, K. Deppert, L. R. Wallenberg, and L. Samuelson, *Nano Lett.* **2**, 87 (2002).

<sup>7</sup>D. Appell, *Nature (London)* **419**, 553 (2002).

<sup>8</sup>L. Samuelson, *Mater. Today* **6**, 22 (2003).

<sup>9</sup>Z. Zhong, D. Wang, Y. Cui, M. W. Bockrath, and C. M. Lieber, *Science* **302**, 1377 (2003).

<sup>10</sup>B. L. Altshuler and A. G. Aronov, *JETP Lett.* **33**, 499 (1981).

<sup>11</sup>G. Bergmann, *Solid State Commun.* **42**, 815 (1982).

<sup>12</sup>S. Hikami, A. I. Larkin, and Y. Nagaoka, *Prog. Theor. Phys.* **63**, 707 (1980).

<sup>13</sup>G. Bergmann, *Phys. Rep.* **107**, 1 (1984).

<sup>14</sup>C. W. J. Beenakker and H. van Houten, *Phys. Rev. B* **38**, 3232 (1988).

<sup>15</sup>D. A. Poole, M. Pepper, and A. Hughes, *J. Phys. C* **15**, L1137 (1982).

<sup>16</sup>J. B. Miller, D. M. Zumbühl, C. M. Marcus, Y. B. Lyanda-Geller, D. Goldhaber-Gordon, K. Campman, and A. C. Gossard, *Phys. Rev. Lett.* **90**, 076807 (2003).

<sup>17</sup>S. A. Studenikin, P. T. Coleridge, N. Ahmed, P. Poole, and A. Sachrajda, *Phys. Rev. B* **68**, 035317 (2003).

<sup>18</sup>D. M. Zumbühl, J. B. Miller, C. M. Marcus, K. Campman, and A. C. Gossard, *Phys. Rev. Lett.* **89**, 276803 (2002).

<sup>19</sup>B. J. Ohlsson, M. T. Björk, A. I. Persson, C. Thelander, L. R. Wallenberg, M. H. Magnusson, K. Deppert, and L. Samuelson, *Physica E (Amsterdam)* **13**, 1126 (2002).

<sup>20</sup>C. Thelander, M. T. Björk, M. Larsson, A. E. Hansen, L. R. Wallenberg, and L. Samuelson, *Solid State Commun.* **131**, 573 (2004).

<sup>21</sup>C. Thelander, T. Mårtensson, M. T. Björk, B. J. Ohlsson, M. W. Larsson, L. R. Wallenberg, and L. Samuelson, *Appl. Phys. Lett.* **83**, 2052 (2003).

<sup>22</sup>L. Samuelson, B. J. Ohlsson, M. T. Björk, and H. Xu, in *Nanowires and Nanobelts Volume 1*, edited by Z. L. Wang (Kluwer, Dordrecht, 2003), p. 69.

<sup>23</sup>We use the 3D expression for the Fermi energy.

<sup>24</sup>Ç. Kurdak, A. M. Chang, A. Chin, and T. Y. Chang, *Phys. Rev. B* **46**, 6846 (1992).

<sup>25</sup>S. Chakravarty and A. Schmid, *Phys. Rep.* **140**, 193 (1986).

<sup>26</sup>T. J. Thornton, M. L. Roukes, A. Scherer, and B. P. Van de Gaag, *Phys. Rev. Lett.* **63**, 2128 (1989).

<sup>27</sup>W. Knap, C. Skierbiszewski, A. Zduniak, E. Litwin-Staszewska, D. Bertho, F. Kobbi, J. L. Robert, G. E. Pikus, F. G. Pikus, S. V. Iordanskii, V. Mosser, K. Zekentes, and Y. B. Lyanda-Geller, *Phys. Rev. B* **53**, 3912 (1996).

<sup>28</sup>G. Dresselhaus, *Phys. Rev.* **100**, 580 (1955).

<sup>29</sup>Y. L. Bychkov and E. I. Rashba, *J. Phys. C* **17**, 6039 (1984).

<sup>30</sup>R. J. Elliott, *Phys. Rev.* **96**, 266 (1954).

<sup>31</sup>J. N. Chazalviel, *Phys. Rev. B* **11**, 1555 (1975).